

## Sign-Singular Measures: Fast Magnetic Dynamos, and High-Reynolds-Number Fluid Turbulence

Edward Ott and Yunson Du

Laboratory for Plasma Research, University of Maryland, College Park, Maryland 20742

K. R. Sreenivasan, A. Juneja, and A. K. Suri

Mason Laboratory, Yale University, New Haven, Connecticut 06520

(Received 3 June 1992)

It is shown that signed measures (i.e., measures that take on both positive and negative values) may exhibit an extreme form of singularity in which oscillations in sign occur everywhere on arbitrarily fine scale. A *cancellation exponent* is introduced to characterize such measures quantitatively, and examples of significant physical situations which display this striking type of singular behavior are discussed.

PACS numbers: 05.45.+b, 47.25.-c, 52.35.-g

Many physical processes have been shown to be described by multifractal *probability measures*. Examples include chaotic dynamical systems [1,2], the dissipation field of fully developed turbulence [3,4], clouds [5], and diffusion-limited aggregation [6]. Briefly, a probability measure  $\mu_p$  on the collection of all subsets of a set  $X$  assigns a non-negative number  $\mu_p(S)$  to any subset  $S$  of  $X$ , satisfies the relation  $\mu_p(\sum_i S_i) = \sum_i \mu_p(S_i)$  for  $\{S_i\}$  any countable collection of disjoint subsets of  $X$ , and assigns the number 1 to  $\mu_p(X)$ . A probability measure is commonly said to be *multifractal* if its generalized dimension spectrum [1]  $D_q$  varies with  $q$ .

In this paper we shall be interested in *signed measures* [7]. In contrast to a probability measure, a signed measure of a set can take on either positive or negative values. Our main point is that signed measures arising in physical situations can be singular in a new way, not present for probability measures. We shall give examples in the context of the theory of kinematic magnetic dynamos, and experimental data from fluid turbulence.

To describe the type of behavior we are interested in, consider the case of a signed measure  $\mu$  on a finite interval  $X$  of the  $x$  axis. Let  $A \subset X$  be an  $x$  interval such that  $\mu(A) \neq 0$ . We say that the measure  $\mu$  is *sign singular* if, for any such interval  $A$  (no matter how small), there is an interval  $B$  contained in  $A$  such that  $\mu(B)$  has the opposite sign from  $\mu(A)$ . Thus the measure  $\mu$  everywhere changes sign on arbitrarily fine scale.

As in the case of multifractals, where the singular nature of a probability measure is quantitatively characterized by its dimension spectrum  $D_q$ , we also desire a means of quantitatively characterizing sign-singular measures. To do this we introduce a quantity, which we call the *cancellation exponent*. Again consider the case of signed measure  $\mu$  on a finite interval  $X$  of the  $x$  axis. Cover the measure with disjoint intervals of equal length  $\epsilon$ . Then we define the cancellation exponent  $\kappa$  by [8]

$$\kappa = \limsup_{\epsilon \rightarrow 0} \frac{\ln \sum_i |\mu(I_i)|}{\ln(1/\epsilon)}, \quad (1)$$

where  $I_i$  denotes the  $i$ th  $\epsilon$ -length interval. For a probability measure,  $|\mu_p(I_i)| \equiv \mu_p(I_i)$ , so that  $\sum |\mu_p(I_i)| = 1$ , and

thus  $\kappa$  is trivially zero. For a signed measure which has a *smooth* bounded density  $\rho(x)$ , we have  $\mu(S) \equiv \int_S \rho(x) dx$ . Thus, when  $\epsilon$  becomes smaller than the smallest characteristic scale for variation of  $\rho(x)$ , then the sum  $\sum |\mu(I_i)|$  approximates the integral  $\int |\rho(x)| dx$ ; hence the sum becomes constant at small  $\epsilon$ , again leading to  $\kappa = 0$ . In order to have positive  $\kappa$ , the sum  $\sum |\mu(I_i)|$  must continue to increase as  $\epsilon$  gets smaller. Since the sum increases only because cancellation of positive and negative contributions is reduced with decreasing  $\epsilon$ , it follows that  $\kappa > 0$  is an indication of oscillation in sign on arbitrarily fine scale [9]. We now wish to show that the above discussion has relevance in physical circumstances.

As our first example, we consider the case of the fast kinematic dynamo problem which addresses the following question: Given a flow of an initially unmagnetized, electrically conducting fluid, will a small seed magnetic field tend to grow exponentially in time? If the answer is yes, then it is unnatural for the flow to exist in the magnetic-field-free state, and one can expect large fields to be generated. Thus the kinematic dynamo problem has been thought to be relevant for explaining why magnetic fields occur in natural objects, such as planets, stars, and galaxies. Motivated by the extremely large conductivity in stars and galaxies, recent interest has attached to the limit where the electrical conductivity of the fluid approaches infinity. If dynamo action is obtained in this limit, one says that the dynamo is *fast* [10]. It has been shown that fast dynamos are connected with flows that are chaotic (e.g., Refs. [11,12], and references therein) in the sense that infinitesimally nearby fluid elements separate exponentially with time. We now present a simple model [12] which captures many of the main qualitative features of typical chaotic fast kinematic dynamos.

We consider deformations of the square,  $0 \leq x \leq 1$ ,  $0 \leq y \leq 1$ , as shown in Fig. 1. The square is first divided into four horizontal strips of widths  $\alpha$ ,  $\beta$ ,  $\gamma$ , and  $\delta$  with  $\alpha + \beta + \gamma + \delta = 1$  [see Fig. 1(a)]. Then each of these is incompressibly squashed horizontally and stretched vertically, so that its vertical length is 1 [Fig. 1(b)]. The strips are then reassembled in the area of the original square with the orientation of the third,  $\gamma$ -width, strip re-

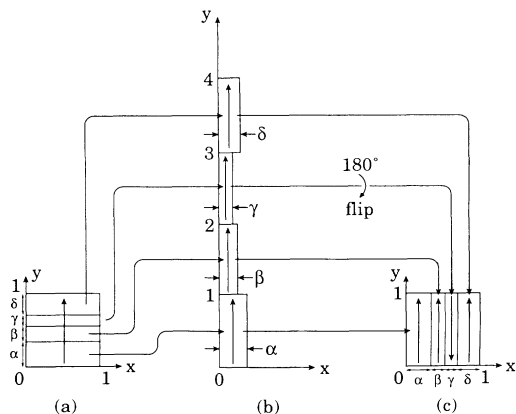


FIG. 1. Four strip baker's map dynamo model.

versed [Fig. 1(c)]. Now we imagine that the two-dimensional  $x$ - $y$  space in which these deformations occur is filled with a perfectly conducting fluid and that an initial magnetic field  $B_0(x)y_0$  exists in the square in Fig. 1(a). Thus the initial magnetic flux through a horizontal line crossing the square is  $\Phi_0 = \int_0^1 B_0(x) dx$ . By the assumption of perfect conductivity of the fluid, the magnetic flux is frozen into the fluid as it deforms. Hence the vertical flux through any of the strips in Fig. 1(b) is still  $\Phi_0$ . (However, since the strips are narrower, their magnetic fields are amplified as compared to the initial field by the factors  $1/\alpha$ ,  $1/\beta$ ,  $1/\gamma$ , and  $1/\delta$  for the first, second, third, and fourth strips, respectively.) The total flux across the square in Fig. 1(c) is thus  $2\Phi_0$ , corresponding to three strips with upward flux and one strip with downward flux [13]. As the sequence of operations in Fig. 1 is successively repeated, the flux across the square doubles on each iterate (dynamo action), and the number of strips quadruples. Thus at iterate  $t$ , the total number of strips is  $4^t$  and the total flux is  $\Phi(t) = \int_0^1 B(x,t) dx = 2^t \Phi_0$ . The magnitude of the flux in each of the  $4^t$  strips is still  $\Phi_0$  by flux conservation. The fact that these  $4^t$  strips only yield a total flux of  $2^t \Phi_0$  indicates that the fluxes of all but a fraction  $2^t/4^t = 2^{-t}$  of the strips are canceling (upward flux strips canceling downward flux strips). Thus, as time proceeds, the fractional cancellation increases exponentially, even though the total flux grows.

The above considerations have been in the context of a perfectly conducting fluid. Finite conductivity leads to diffusion of the magnetic field. To include this resistive diffusion, we assume that the deformations of the square are done impulsively, so that no diffusion takes place during the actions shown in Fig. 1. However, after each deformation the fluid lies stationary for one time unit before the deformation is again applied [12]. Between deformations,  $B(x,t)$  evolves according to the diffusion equation  $\partial B/\partial t = R_m^{-1} \partial^2 B/\partial x^2$ , where  $R_m$  is the "magnetic Reynolds number" for our model and may be thought of as a normalized electrical conductivity. For typical initial

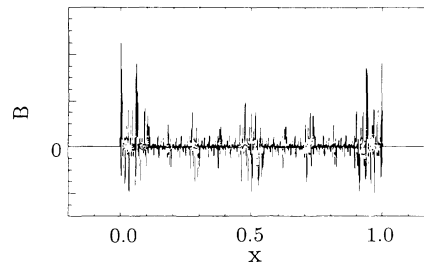


FIG. 2. The final spatial distribution of magnetic field,  $B(x)$  vs  $x$ , for  $R_m = 10^7$ ,  $\alpha = \delta = \frac{7}{16}$ ,  $\beta = \gamma = \frac{1}{16}$ .

conditions,  $B_0(x)$ , the temporal evolution of the magnetic field, after a transient phase, eventually settles into a final spatial  $x$  dependence corresponding to the eigenfunction of the largest exponential growth rate. Balancing the temporal exponential decrease of spatial scale of  $B(x,t)$  (inherent in the map process; Fig. 1) with the diffusive smoothing between deformations of the square leads to an estimate of  $R_m^{-1/2}$  for the minimum spatial scale of the final magnetic-field distribution. (This result applies generally for fast dynamos and is not limited to the model in Fig. 1.) Thus, as  $R_m$  is increased, we expect wilder and wilder variation in the final spatial distribution. Figure 2 shows numerical results for such a one-dimensional distribution [8] (cf. Ref [12]) for  $\alpha = \delta = \frac{7}{16}$ ,  $\beta = \gamma = \frac{1}{16}$ , and  $R_m = 10^7$ . (For comparison note that the magnetic Reynolds number on the surface of the Sun is  $\sim 10^9$ .) In the fast dynamo limit,  $R_m \rightarrow \infty$ , the final magnetic field approaches a measure which, as shown below, is sign singular.

To illustrate this, consider the special case of equal width strips  $\alpha = \beta = \gamma = \delta = \frac{1}{4}$ . Divide the interval  $0 \leq x \leq 1$  into  $4^k$  subintervals of length  $\epsilon = 4^{-k}$ . Assuming  $\epsilon > R_m^{-1/2}$ , the flux through any one of these subintervals normalized by the total flux  $\Phi(t) = 2^t \Phi_0$  ( $t$  an integer) becomes independent of time for  $t \geq k$  and is either  $+2^{-k}$  or  $-2^{-k}$ . Using the normalized flux as our measure, we have  $|\mu(I_i)| = 2^{-k}$ , where  $I_i$  denotes one of the  $\epsilon = 4^{-k}$  length intervals. Thus  $\sum |\mu(I_i)| = 4^k 2^{-k} = 2^k$ , and (1) yields  $\kappa = \frac{1}{2}$ . Hence  $\kappa > 0$ , consistent with the measure being sign singular (for scales larger than  $R_m^{-1/2}$ ). In the more general case of unequal  $\alpha$ ,  $\beta$ ,  $\gamma$ , and  $\delta$ , utilization of the self-similar nature of the model yields  $\kappa$  (independent of  $R_m$ ) as the solution of the following transcendental equation [8]:  $\alpha^\kappa + \beta^\kappa + \gamma^\kappa + \delta^\kappa = 2$ . Figure 3(a) shows a plot of  $\ln \sum |\mu(I_i)|$  vs  $\ln(1/\epsilon)$  obtained by numerical time evolution of our model ( $\alpha = \delta = \frac{7}{16}$ ,  $\beta = \gamma = \frac{1}{16}$ ,  $R_m = 10^{10}$ ). The slope of the fitted line yields  $\kappa = 0.43$  in agreement with the theoretical result. Note in Fig. 3(a) the cutoff of the  $\kappa$  scaling range at small  $\epsilon$  due to resistive magnetic diffusion. (A similar plot for  $R_m = 10^7$ , corresponding to Fig. 2, also yields  $\kappa \cong 0.43$ , but with a smaller scaling range consistent with the predicted cutoff at  $\epsilon \sim R_m^{-1/2}$ .)

The above result for our simple model, Fig. 1, is quan-

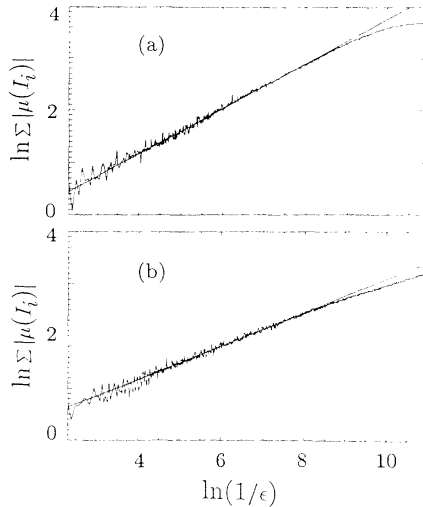


FIG. 3.  $\ln \sum |\mu(I_i)|$  vs  $\ln(1/\epsilon)$  (a) for the model of Fig. 1 with  $R_m = 10^{10}$ , and (b) for a particular spatially smooth three-dimensional chaotic fluid flow.

tatively similar to results for a spatially smooth, chaotic, incompressible, three-dimensional flow. In particular, we consider the example of a velocity field

$$\mathbf{v}(\mathbf{x}, t) = [\hat{v}_x(\mathbf{x})\Delta(t)\mathbf{x}_0 + \hat{v}_y(\mathbf{x})\Delta(t - \eta)\mathbf{y}_0 + \hat{v}_z(\mathbf{x})\Delta(t - 2\eta)\mathbf{z}_0],$$

where  $\hat{v}_x(\mathbf{x}) = 1.5(\sin x + \cos y)$ ,  $\hat{v}_y(\mathbf{x}) = 1.5(\sin x + \cos z)$ ,  $\hat{v}_z(\mathbf{x}) = 1.5(\sin y + \cos x)$ ,  $\Delta = \sum_j \delta(t - j)$ , and  $\eta$  is a number between 0 and  $\frac{1}{2}$ . Figure 3(b) shows [14] a plot of  $\ln \sum |\mu(I_i)|$  vs  $\ln(1/\epsilon)$ . In this case we calculate the  $y$  component of the magnetic field on a vertical line segment through a randomly chosen point on the  $z = 0$  plane (the same result is obtained for other line segments). The cancellation exponent from Fig. 3(b) is  $\kappa \cong 0.31$ .

As our second example, consider a blob of vorticity in a high-Reynolds-number turbulent flow. The blob will be stretched, folded, and rearranged during its dynamical evolution. Eventually, a section through the vorticity field will yield a graph which displays high spatial variability of both signs. The similarity of the rearrangement process to that in the dynamo problem suggests that a cancellation exponent can be determined for the vorticity fluctuations. Similar features can be expected also of other rapidly oscillating properties such as velocity derivatives.

To test this notion, measurements were made in several fully turbulent flows. We obtained streamwise components of velocity in the atmospheric surface layer at a height of about 18 m above the ground (2 m above the roof of a four-story building). The mean wind speed  $U$  was about 6 m/s and the microscale Reynolds number  $R_\lambda$  was about 1500. Additional measurements of velocity were also made at a height of 6 m above the ground over a wheat field in an open field. The mean wind speed was 4 m/s and the microscale Reynolds number  $R_\lambda$  was about

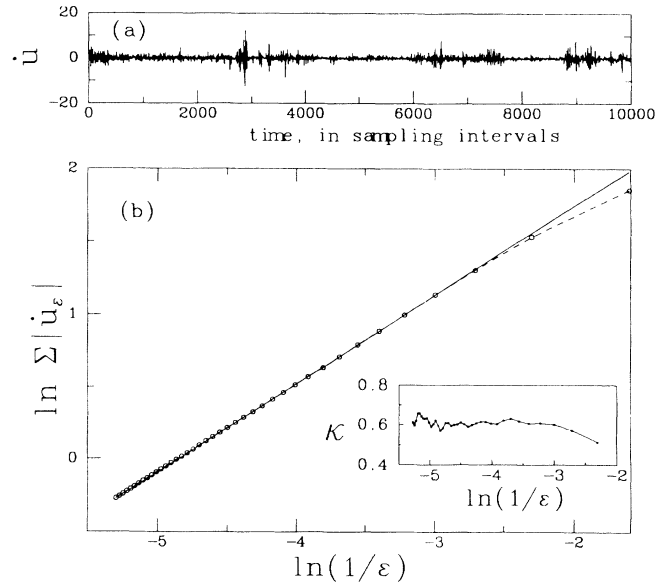


FIG. 4. (a) A typical trace of the velocity derivative as a function of time, in units of the root-mean square of the signal. (b) A plot of  $\ln \sum |\dot{u}_\epsilon|$  vs  $\ln(1/\epsilon)$ . A reasonably good power-law fit is possible, as seen in the inset which gives the local slope  $\kappa$ . The cutoff for small  $\epsilon$  in (b) is consistent with the cutoff due to viscous diffusion.

2000. These measurements were made with single hot wires (0.6 mm in length and  $0.5 \mu\text{m}$  in diameter) operated on DANTEC anemometers in the constant temperature mode. A temporal trace of streamwise velocity fluctuations was obtained at a single "point" in the flow by digitizing anemometer signals with 12-bit resolution at a sampling rate that varied between 6000 and 10000 Hz. This sampling rate is adequate to resolve Kolmogorov scales in the flow. The record length varied between 140 000 and 800 000 points.

In addition, in another set of experiments, the velocity field in a plane was obtained in the turbulent wake of a circular cylinder at several moderate Reynolds numbers by the use of particle image velocimetry (PIV). The technique consists of seeding the flow with small particles whose positions at two closely spaced intervals were captured on photographic film by using laser pulses. The photographic film was developed and interrogated by a light beam from a low-powered He-Ne laser. The information from the resulting Young's fringes is converted to vector data using the software purchased from FFD, Inc. Further experimental details and a discussion of the accuracy of measurements can be found in Ref. [15].

As expected, the velocity field itself yields a trivial value zero for the cancellation exponent. On the other hand, quantities such as velocity derivatives and vorticity yield nontrivial values, and we expect these values to be universal for high-Reynolds-number turbulent flows. We first show this for our atmospheric flow data. For a given  $\epsilon$  interval let  $\dot{u}_\epsilon = \sum (\Delta u / \Delta t)$ , where  $\Delta u$  represents the velocity difference over one sampling interval in the digi-

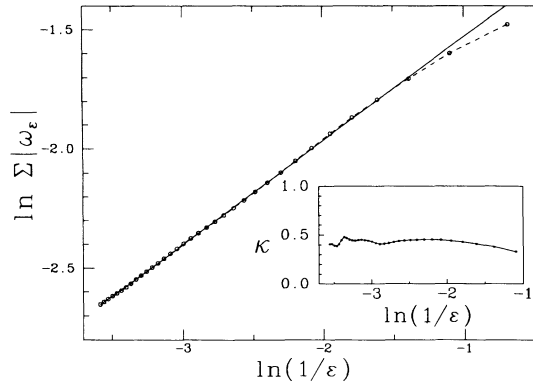


FIG. 5. A plot of  $\ln \Sigma |\omega_\epsilon|$  vs  $\ln(1/\epsilon)$  for the vorticity component  $\omega_y$  in the far field of the cylinder wake.

tized record of the velocity trace, and the summation extends over all digitized points in the  $\epsilon$  interval. In Fig. 4 we plot  $\ln \Sigma |\dot{u}_\epsilon|$  vs  $\ln(1/\epsilon)$ , with the summation extending over all  $\epsilon$  intervals [16]. The figure shows that there is a good scaling region of about a decade and that the cancellation exponent is approximately 0.6.

We have also computed the  $y$  component of the vorticity  $\omega_y$  from our data for the wake behind a circular cylinder, where  $x$  is the streamwise direction and  $y$  is perpendicular to the axis of the cylinder. The resolution of the velocity measurement is on the order of 1.5 Kolmogorov scales at the cylinder Reynolds number of 1100. Analogously to  $\dot{u}_\epsilon$ , we define  $\omega_\epsilon = \Sigma \omega_y$  (where the sum is over points in the  $\epsilon$  interval) and then examine the  $\epsilon$  scaling of  $\Sigma |\omega_\epsilon|$  (where the sum is over  $\epsilon$  intervals). For direct comparison with velocity derivatives, the vorticity along lines of constant  $x$  were strung together to give a one-dimensional string of data. Figure 5 shows that a decent scaling exists, and yields a cancellation exponent of 0.45 [17].

In conclusion, we have shown that sign-singular measures with nontrivial cancellation exponents occur in dynamos and fluid turbulence, and we expect that this may prove to be true in many other physical situations.

The work at the University of Maryland was supported by the Office of Naval Research (Physics). The work at Yale was supported by a grant from DARPA.

- [1] P. Grassberger and I. Procaccia, *Physica* (Amsterdam) **9D**, 189 (1983).  
 [2] J. D. Farmer, E. Ott, and J. A. Yorke, *Physica* (Amsterdam) **7D**, 153 (1983); P. Grassberger, *Phys. Lett.* **107A**, 101 (1985); T. C. Halsey, M. H. Jensen, L. P. Kadanoff, I. Procaccia, and B. I. Shraiman, *Phys. Rev. A* **37**, 1711 (1988).  
 [3] B. Mandelbrot, *J. Fluid Mech.* **62**, 331 (1974); R. Benzi, G. Paladin, G. Parisi, and A. Vulpiani, *J. Phys. A* **17**, 3521 (1984); U. Frisch and G. Parisi, in *Turbulence and Predictability in Geophysical Fluid Dynamics and Climate Dynamics*, edited by M. Ghil, R. Benzi, and G. Par-

isi (North-Holland, New York, 1985), p. 84.

- [4] K. R. Sreenivasan and C. Meneveau, *Phys. Rev. A* **38**, 6287 (1988); C. Meneveau and K. R. Sreenivasan, *J. Fluid Mech.* **224**, 429 (1991); K. R. Sreenivasan, *Annu. Rev. Fluid Mech.* **23**, 539 (1991).  
 [5] S. Lovejoy, D. Schertzer, and A. A. Tsonis, *Science* **235**, 1036 (1987).  
 [6] C. Amitrano, C. Coniglio, and F. DiLiberto, *Phys. Rev. Lett.* **57**, 1016 (1986).  
 [7] P. R. Halmos, *Measure Theory* (Norstrand, New York, 1962), Chap. 6.  
 [8] Y. Du and E. Ott, "Dimensions of Fast Dynamo Magnetic Field" (to be published).  
 [9] We emphasize that physical signed measures have smooth densities because of small scale cutoffs (like the Kolmogorov microscale), so that  $\kappa$  in physical cases is meaningful only if a scaling range of  $\Sigma |\mu(I_i)|$  exists for  $\epsilon$  sufficiently small but still larger than the cutoff. We also note that although we have been considering the signed measure  $\mu$  to be on an interval of the  $x$  axis, the discussion easily generalizes to measures on areas or volumes. For example, for the case of an area, the sets  $I_i$  in the definition of  $\kappa$ , Eq. (1), becomes squares of edge length  $\epsilon$ . Another generalization of (1) is to consider  $\limsup_{\epsilon \rightarrow 0} \ln \Sigma |\mu(I_i)|^q / \ln(1/\epsilon)$ . This will be discussed in a future publication where we also plan to consider correlation functions associated with signed measures.  
 [10] S. I. Vainshtein and Ya. B. Zeldovich, *Usp. Fiz. Nauk* **106**, 431 (1972) [*Sov. Phys. Usp.* **15**, 159 (1972)].  
 [11] V. I. Arnold, Ya. B. Zeldovich, A. A. Ruzmaikin, and D. D. Sokolov, *Zh. Eksp. Teor. Fiz.* **81**, 2052 (1981) [*Sov. Phys. JETP* **54**, 1083 (1981)]; D. Galloway and U. Frisch, *Geophys. and Astrophys. Fluid Dyn.* **36**, 53 (1986); B. J. Bayly and S. Childress, *ibid.*, **44**, 211 (1988); J. M. Finn and E. Ott, *Phys. Fluids* **31**, 2992 (1988).  
 [12] J. M. Finn and E. Ott, *Phys. Fluids B* **2**, 916 (1990).  
 [13] We imagine that the field lines in Fig. 1(b) are cut at  $y=1, 2$ , and 3 before the strips are reassembled into the square [Fig. 1(c)].  
 [14] For Fig. 3(b) the magnetic field is calculated for the case of a perfectly conducting fluid. This greatly facilitates the computation [11], and should not affect the result for  $\kappa$  [8] (e.g., this can be rigorously shown to be so for the model of Fig. 1). In the computation, an initial uniform vertical magnetic field was evolved from  $t=0$  to 20 and the  $t=20$  result was used to obtain Fig. 3(b). The turnover in Fig. 3(b) at  $\ln(1/\epsilon) \approx 8.5$  occurs at a later time as the iteration time is increased. This is because the smallest generated scale size decreases exponentially with time as a result of the chaos of the flow.  
 [15] A. Juneja, A. M. Migdal, K. R. Sreenivasan, A. K. Suri, and V. Yakhot (to be published).  
 [16] Since  $\dot{u}_\epsilon$  is the integral of  $\dot{u}$  over a time interval  $\epsilon$ , it is just the difference of  $u$  at two times separated by  $\epsilon$ . Thus in this case  $\kappa$  is the order 1 velocity structure function.  
 [17] The streamwise component of velocity was also measured in the atmosphere with a four-wire configuration of hot wires [M. S. Fan, Ph.D. thesis, Yale University, 1991 (unpublished)], but the data do not yield constant scaling over a sizable range. The reasons for this behavior are not clear.